УДК 621.315.592

# Structural and electronic properties of $Si_{1-x}Ge_x$ binary semiconducting alloys under the effect of temperature and pressure

© A.R. Degheidy, E.B. Elkenany¶

Department of Physics, Faculty of Science, Mansoura University,
35516 Mansoura, Egypt

(Получена 7 ноября 2012 г. Принята к печати 8 ноября 2012 г.)

Based on the empirical pseudo-potential method which incorporates compositional disorder as an effective potential, the band structure of $Si_{1-x}Ge_x$ alloy are calculated for different alloy composition $x$. The effect of temperature and pressure on the electronic band structure of the considered alloy has been studied. Monotonic decreasing and increasing functions are obtained for the temperature and pressure dependent form factors respectively. Some physical quantities as band gaps, bowing parameters, and the refractive index of the considered alloy with different Ge concentration and under the effect of temperature and pressure are calculated. The results obtained are found in good agreement with the experimental and published data.

## 1. Introduction

Semiconductor alloys plays an important role in the nanotechnology science and enter in the design of the optoelectronic devices. Most of alloys have become important components of the optoelectronic devices such as light emitting and laser diodes (LEDs and LDs) in green, blue, and UV regime [1].

There has been a strong revival of interest in the electronic properties of $Si_{1-x}Ge_x$ alloys in the context of super lattice physics [2–4]. Therefore, the investigation of the electronic band structure of $Si_{1-x}Ge_x$ alloys has attracted considerable interest. They offer the freedom to design material properties by choosing appropriate alloy constituents. We consider in this work the binary semiconducting alloy $Si_{1-x}Ge_x$ which has received extensive attention, as reflected by the recent experimental, theoretical, and numerical studies.

Therefore, the investigation of the electronic band structure of $Si_{1-x}Ge_x$ alloys has attracted considerable interest. The investigation of the pressure and temperature dependence of the energy gaps in semiconductors has been the subject of many studies in the past three decades [5–13]. In the present work we study the effect of temperature from (0 to 500 K) and pressure from (0 to 120 kbar) on the electronic band structure and some optoelectronic properties specifically, the energy band gaps, refractive index, and dielectric constant at high-symmetry points in $Si_{1-x}Ge_x$ alloys. Monotonic decreasing and increasing functions are obtained for temperature and pressure dependent form factors respectively. Our calculations are based on the local pseudopotential method under the virtual crystal approximation in which the effect of compositional disorder is involved. The present calculations are performed by using an own routine based on the MATLAB program which based on 65 reciprocal lattice vector $\mathbf{G}$ [14–17].

¶ E-mail: kena@mans.edu.eg

## 2. Theory and calculations

The electronic structure of an alloy has been calculated using the empirical pseudo-potential method (EMP) [18,19]. The alloy potential $\mathbf{V}(\mathbf{r})$ is calculated within the virtual crystal approximation $\mathbf{V}_{\mathrm{VCA}}(\mathbf{r})$ which is a periodic potential and a non-periodic potential $V_{\mathrm{dis}}(r)$ due to the compositional disorder [20–22]:

$$\mathbf{V}(\mathbf{r}) = \mathbf{V}_{\mathrm{VCA}}(\mathbf{r}) + \mathbf{V}_{\mathrm{dis}}(\mathbf{r}), \tag{1}$$

$\mathbf{V}_{\mathrm{VCA}}(\mathbf{r})$ and $\mathbf{V}_{\mathrm{dis}}(\mathbf{r})$ could be written as [20–22]

$$\mathbf{V}_{\mathrm{VCA}}(\mathbf{r}) = x\mathbf{V}_{\mathrm{Ge}}(\mathbf{r}) + (1-x)\mathbf{V}_{\mathrm{Si}}(\mathbf{r}), \tag{2}$$

$$\mathbf{V}_{\mathrm{dis}}(\mathbf{r}) = -\Omega\sqrt{x(1-x)}\big[\mathbf{V}_{\mathrm{Si}}(\mathbf{r}) - \mathbf{V}_{\mathrm{Ge}}(\mathbf{r})\big], \tag{3}$$

where $\Omega$ is treated as an adjustable parameter which equal to zero when the disorder effect is neglected, and $x$ is the Ge concentration.

The potential of a pure semiconductors element, $\mathbf{V}(\mathbf{r})$, could be expanded in terms of reciprocal lattice vectors $\mathbf{G}$ as [18]:

$$V(G) = \sum_{G \neq G'} a_{nk}(\mathbf{G}')\big[W^s(\Delta\mathbf{G})\cos(\Delta\mathbf{G}\cdot\tau) + iW^A(\Delta\mathbf{G})\sin(\Delta\mathbf{G}\cdot\tau)\big], \tag{4}$$

where $W^s$ and $W^A$ are the symmetrical and antisymmetrical form factors respectively, $\Delta\mathbf{G} = |\mathbf{G} - \mathbf{G}'|$, $G$ and $G'$ are the reciprocal lattice vectors; $\tau = (a/8)\,(1,1,1)$ is the position vector of each atom in the unit cell and a is the lattice constant.

The final expression for the pseudo-potential form factors of the alloy $Si_{1-x}Ge_x$ could be taken as [20–22]

$$W^{S,A} = xW^{S,A}_{\mathrm{Ge}} + (1-x)W^{S,A}_{\mathrm{Si}} - \Omega\sqrt{x(1-x)}\big[W^{S,A}_{\mathrm{Si}} - W^{S,A}_{\mathrm{Ge}}\big], \tag{5}$$

where $W^{S,A}_{\mathrm{Si}}$ and $W^{S,A}_{\mathrm{Ge}}$ are the form factors of the pure Si and pure Ge respectively.

The adjustable parameter $\Omega$ is found in the disorder part in Eq. (5) which is adjusting to give good agreement with the experimental data. When the VCA is used alone (without taking into account the disorder effect), $\Omega$ equals to zero. However, when the compositional disorder is included, the value of $\Omega$ is ranged about 0.459.

The lattice constant of the alloy is obtained according to Vegard's rule [23] by

$$a_{Si_{1-x}Ge_x} = (1-x)a_{Si} + x a_{Ge}, \tag{6}$$

where $a_{Si}$ and $a_{Ge}$ are the lattice constants of the elements Si and Ge respectively.

The electronic energy spectra of Si and Ge have been calculated by using the local pseudo-potential method. The form factors of these elements are adjusted to give good agreement between the calculated energy gaps and the corresponding experimental value at high symmetry points in the Brillouin zone. Once the associated semiconductor form factors of Si and Ge are determined, then calculations are done to solve for the band structure. The eigenvalues and the eigenvectors are found by solving the matrix Eq. (7)

$$\frac{h^2}{2m}|\mathbf{k}+\mathbf{G}'|^2 A_{n,\mathbf{k}}(\mathbf{G}',x) + \sum_{\mathbf{G}\neq\mathbf{G}'} A_{n,\mathbf{k}}(\mathbf{G}',x), V\big(|\mathbf{G}-\mathbf{G}'|,x\big) = E_{nk}(x)A_{n,\mathbf{k}}(\mathbf{G}',x), \tag{7}$$

where $\hbar$ is the Plank constant, $\mathbf{G}$ are the reciprocal lattice vectors, $k$ is the wave vector, $m$ is the mass of electron, $V(|\mathbf{G}-\mathbf{G}'|)$ is given in Eq. (5) or solving the secular determinant [5]

$$\left\| \frac{1}{2}|\mathbf{k}+\mathbf{G}'|^2 - E_{n\mathbf{k}}(x) + \sum_{\mathbf{G}\neq\mathbf{G}'} V(|\mathbf{G}-\mathbf{G}'|,x) \right\| = 0. \tag{8}$$

For different composition $x$ and by varying the adjustable parameter $\Omega$ until agreement was achieved with the experiments. Since the aim is to study in the effects of temperature $T$ and pressure $P$ beside the compositional effect $x$ on the electronic structure of the alloy, Eqs (7), (8) could be written in general forms as

$$\frac{h^2}{2m}|\mathbf{k}+\mathbf{G}'|^2 A_{n,\mathbf{k}}(\mathbf{G}',x,Z) + \sum_{\mathbf{G}\neq\mathbf{G}'} A_{n,\mathbf{k}}(\mathbf{G}',x,Z) \times V\big(|\mathbf{G}-\mathbf{G}'|,x,Z\big) = E_{nk}(x,Z)A_{n,\mathbf{k}}(\mathbf{G}',x), \tag{9}$$

$$\left\| \frac{1}{2}|\mathbf{k}+\mathbf{G}'|^2 - E_{n\mathbf{k}}(x,Z) + \sum_{\mathbf{G}\neq\mathbf{G}'} V\big(|\mathbf{G}-\mathbf{G}'|,x,Z\big) \right\| = 0, \tag{10}$$

where $Z$ may be $T$ or $P$.

Eq. (10) could be solved numerically to give the required eigenvalues for each $k$ and at constant $x, Z$. Arranging the obtained eigenvalues and set the top of the valence bands to zero energy and determines the energy gaps at high symmetry points in the Brillouin zone.

Comparing the calculated energy gaps with the corresponding experimental values, and adjusting the form factors until we obtain the best values of the energy gaps. From these calculated energy gaps of the alloy, some physical properties such as the refractive index of the considered alloy can be obtained.

The refractive index has been calculated using three different models that are related directly to the energy band-gap $E_g$ [24].

1. The Moss formula based on atomic model [25], in which the refractive index is given by

$$n = \sqrt[4]{\frac{\theta}{E_g}}, \tag{11}$$

where $E_g$ is the energy band gap and $\theta$ is a constant equal to 108 eV [26].

2. The Ravindra et al. expression [27], in which $n$ is given by

$$n + \alpha + \beta E_g \tag{12}$$

with $\alpha = 4.084$ and $\beta = -0.62\,(\text{eV})^{-1}$.

3. The empirical relation of Herve and Vandamme [28]

$$n = \sqrt{1 + \left(\frac{A}{E_g + B}\right)^2} \tag{13}$$

with $A = 13.6$ eV and $B = 3.4$ eV, where $n \equiv n(x, Z)$.

## 3. Results and discussion

### 3.1. Effect of Ge concentration on $E_{nk}$ at constant temperature and Pressure

The calculations of the energy band structures based on the local EPM for $Si_{1-x}Ge_x$ alloy is performed by a routine based on the MATLAB language [14].

Table 1 listed the adjusted symmetrical form factors, ($W_3^s$, $W_8^s$, $W_{11}^s$) and the lattice constant of the alloy $Si_{1-x}Ge_x$, for different $x$, $(0 \le x \le 1)$ at constant $Z$ ($T = 0$ K and $P = 0$ kbar).

Tables 2 and 3 show the direct and indirect energy gaps at normal pressure for different alloy composition of $Si_{1-x}Ge_x$ at $T = 0$ and 300 K respectively. The results are compared with the corresponding published data [29–33] which show good agreement.

In Fig. 1 we plot the computed electron energy band structure of $Si_{1-x}Ge_x$ along the high symmetry direction in the Brillouin zone at $T = 0$ K and $P = 0$ kbar for two different values of Ge concentrations, $x = 0.1$ (solid line) and $x = 0.9$ (dashed line). From this Figure we show that the first conduction energy band is more affected by composition than the other bands and exhibits more enhancement at the point $\Gamma$ than any other point $k$ in the Brillouin zone. The energy shifts the calculated energy bands from $x = 0.1$ and $x = 0.9$ are about 2427.1 meV at

**Table 1.** The adjusted symmetric form factors, ($W_3^s$, $W_8^s$, $W_{11}^s$) and lattice constants for $Si_{1-x}Ge_x$ alloy at $T = 0$ K, and $P = 0$ kbar

| $x$<br>Form factors<br>(Ryd) | 0<br>(Si) | 0.1 | 0.3 | 0.5 | 0.7 | 0.9 | (Ge)<br>1 |
|---|---|---|---|---|---|---|---|
| $W_3^s$ | −0.2379777 | – | – | – | – | – | – |
| | – | 0.2526042 | 0.2693807 | 0.2828663 | 0.2939940 | 0.3018309 | 0.2995111 |
| $W_8^s$ | 0.0573077 | 0.0620958 | 0.0675877 | 0.0720024 | 0.0756451 | 0.0782106 | 0.0774512 |
| $W_{11}^s$ | 0.0660302 | 0.0507445 | 0.0332119 | 0.0191184 | 0.0074891 | – | 0.0017234 |
| | – | – | – | – | – | 0.0007010 | – |
| | 5.4267378[m] | 5.4488780[q] | 5.4931585[q] | 5.5374390[q] | 5.5817194[q] | 5.6259999[q] | 5.6481401[m] |

*Notes.* [m] Ref. [19], [q] Rev. [23].

**Table 2.** The direct and indirect energy band gaps for $Si_{1-x}Ge_x$ alloy at $T = 0$ K, and $P = 0$ kbar

| $Si_{1-x}Ge_x$<br>$T = 0$ K | $E_g^L$ (eV) | $E_g^x$ (eV) | $E_g^\Gamma$ (eV) |
|---|---|---|---|
| (Si) | 2.0433 | 1.2546<br>1.17[e] | 3.3304 |
| $Si_{0.1}Ge_{0.9}$ | 1.7621 | 1.2309 | 3.1733 |
| $Si_{0.3}Ge_{0.7}$ | 1.4194 | 1.2024 | 2.3847 |
| $Si_{0.5}Ge_{0.5}$ | 1.1242 | 1.1656 | 1.7145 |
| $Si_{0.7}Ge_{0.3}$ | 0.8712 | 1.1293 | 1.1499 |
| $Si_{0.9}Ge_{0.1}$ | 0.6969 | 1.1140 | 0.7462 |
| (Ge) | 0.7817<br>0.744[e] | 1.1749 | 0.8655 |

*Note.* [e] Ref. [29].

**Table 3.** The direct and indirect energy band gaps for $Si_{1-x}Ge_x$ alloys at $T = 300$ K, and $P = 0$ kbar

| $Si_{1-x}Ge_x$<br>$T = 300$ K | $E_g^L$ (eV) | $E_g^x$ (eV) | $E_g^\Gamma$ (eV) |
|---|---|---|---|
| (Si) | 2.0486 | 1.2645, 1.2091[d],<br>1.3[c], 1.1[e] | 3.3324, |
| | 2.01[a] | | 3.37[b] |
| $Si_{0.1}Ge_{0.9}$ | 1.7677 | 1.2413 | 3.1753 |
| $Si_{0.3}Ge_{0.7}$ | 1.4258 | 1.2139 | 2.3847 |
| $Si_{0.5}Ge_{0.5}$ | 1.1313 | 1.1782 | 1.17144 |
| $Si_{0.7}Ge_{0.3}$ | 0.8790 | 1.1428 | 1.1497 |
| $Si_{0.9}Ge_{0.1}$ | 0.7052 | 1.1284 | 0.7459 |
| (Ge) | 0.7905, 0.74[b],<br>0.66[e], 0.7010[d] | 1.1900<br>1.26° | 0.8652<br>0.89[b] |

*Note.* [a] Ref. [30]; [b] Ref. [31]; [c] Ref. [32]; [d] Ref. [29]; [e] Ref. [34].

point Γ, 1065.2 meV at the point $L$, and 116.9 meV at the point $X$.

The dependence of the direct and indirect band gaps ($E_g^\Gamma$, $E_g^L$ and $E_g^X$) on the alloy composition for $Si_{1-x}Ge_x$ alloys at $T = 0$ K and $P = 0$ kbar is shown in Fig. 2. The energy gaps, $E_g^\Gamma$, $E_g^L$, and $E_g^X$ decreasing from 3.3304, 2.0433, and 1.2546 eV at $x = 0$ to 0.8655, 0.7817, and 1.1749 eV at $x = 1$, respectively. The alloy has two crossovers energy, the first from Γ to $X$ points at about $x = 0.76$ and energy 1.19 eV, and secondly from $L$ to $X$ points at about $x = 0.45$ and energy 1.17 eV.

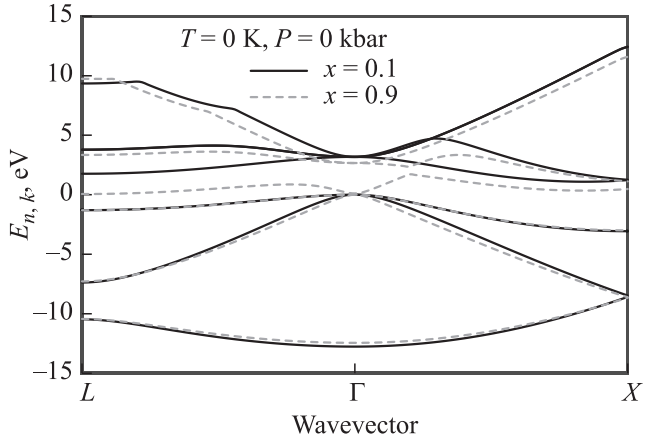


**Figure 1.** The electronic structure of $Si_{1-x}Ge_x$ at $T = 0$ K and $P = 0$ kbar for two different values of Ge concentrations, $x = 0.1$ (solid line) and $x = 0.9$ (dashed line).

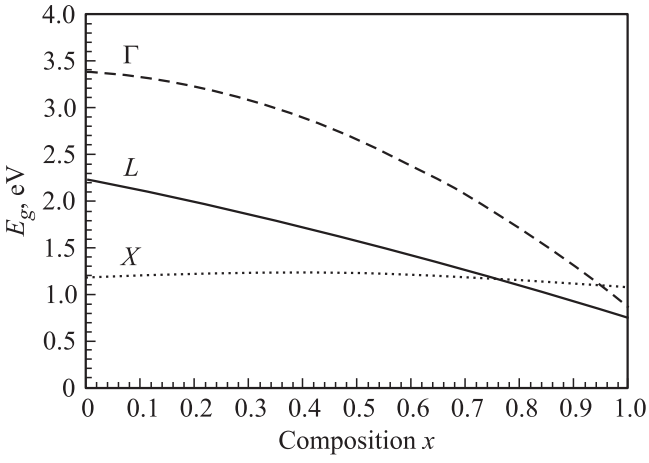


**Figure 2.** The direct and indirect energy band gaps for $Si_{1-x}Ge_x$ at $T = 0$ K, and $P = 0$ kbar.

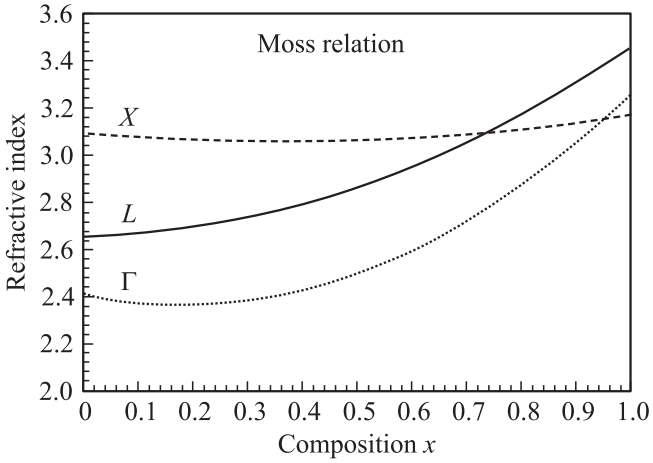


**Figure 3.** The direct and indirect energy band gaps for $Si_{1-x}Ge_x$ at $T = 300\,K$, and $P = 0\,kbar$.

Fig. 3 shows the direct and indirect energy gaps as function of Ge concentration at $T = 300\,K$ and $P = 0\,kbar$. The effect of variation on Ge concentration in the $E_g^{\Gamma}$, $E_g^L$, and $E_g^X$ shows decreasing from 3.3324, 2.0486, and 1.2645 eV at $x = 0$ to 0.8652, 0.7905, and 1.19 eV at $x = 1$, respectively. The $Si_{1-x}Ge_x$ system goes over from a direct band gap to an indirect one at $X$ point, this crossover occurs at about $x = 0.73$, and at energy 1.15 eV, and goes over from an indirect band gap at $L$ point to an indirect one at $X$ point, this crossover occurs at about $x = 0.45$, and at energy 1.2 eV.

**Table 4.** The bowing parameters and $\Gamma-X$ crossover point for $Si_{1-x}Ge_x$ alloys at $T = 300\,K$ and $P = 0\,kbar$

| | Bowing parameter (eV) | $\Gamma-X$ crossover ($x$) |
|---|---|---|
| Present work | 0.1733 | 0.73 |
| Experimental data | 0.21[a] | 0.85[f] |
| Other calculations | 0.169[h], 0.0[g] | 0.87[i], 0.75[g] |

*Notes.* [a] Ref. [30]; [f] Ref. [34]; [i] Ref. [35]; [h] Ref. [36]; [g] Ref. [37].

**Table 5.** The refractive index for $Si_{1-x}Ge_x$ alloys at $T = 300\,K$, and $P = 0\,kbar$

| Composition $n$ | Relation (11) | Relation (12) | Relation (13) |
|---|---|---|---|
| Si | 3.0400 | 3.0824 | 3.3000, 3.46[k] |
| $Si_{0.9}Ge_{0.1}$ | 3.0541 | 3.0962 | 3.3144 |
| $Si_{0.7}Ge_{0.3}$ | 3.0712 | 3.0962 | 3.3314 |
| $Si_{0.5}Ge_{0.5}$ | 3.0942 | 3.1344 | 3.3535 |
| $Si_{0.3}Ge_{0.7}$ | 3.1179 | 3.1563 | 3.3755 |
| $Si_{0.1}Ge_{0.9}$ | 3.1278 | 3.1654 | 3.3844 |
| Ge | 3.4189 | 3.3960 | 3.5939, 4.00[k] |

*Note.* [k] Ref. [7].

A best fit of direct and indirect energy gaps yields:

$$E_g^{\Gamma} = 3.3324 - 3.7985x + 1.1838x^2, \quad (14)$$

$$E_g^X = 1.2645 - 0.2749x + 0.1733x^2, \quad (15)$$

$$E_g^L = 2.0486 - 2.4883x + 1.184x^2. \quad (16)$$

Table 4 displays a comparison for the values of the bowing parameters and the $\Gamma-X$ crossover energy of the Germanium content for the $Si_{1-x}Ge_x$ alloy with the associated published values at nearly room temperature, $T = 300\,K$ and normal atmospheric pressure, $P = 0\,kbar$. It can be seen from Table 4 and Eq. (16) that the present results for the bowing parameters and the $\Gamma-X$ crossover of the Germanium concentration are in close agreement with the published data [30,34–37].

Table 5 lists that the refractive index for $Si_{1-x}Ge_x$ alloys at $T = 300\,K$, and $P = 0\,kbar$. We note that the refractive index is increased with increasing the composition. The present data of refractive index for Si and Ge are in sufficient agreement with the published data. It seen that from Table 5 that the refractive index which calculated from relation (13) is more accurate than the other two relations.

### 3.2. Effect of temperature $T$ on $E_{nk}$ at constant composition $x$ and pressure $P$

For a given composition parameter $x$, and a constant pressure $P = 0\,kbar$ the temperature dependent eigenvalues and eigenvectors are found by solving the secular determinant,

$$\left\| \frac{1}{2}\left|\vec{k} + \vec{G}'\right|^2 - E_{nk}(T) + \sum_{G \neq G'} V\left(\left|\Delta\vec{G}\right|, T\right) \right\| = 0, \quad (17)$$

where

$$V\left(\left|\Delta\vec{G}\right|, T\right) = W^s\left(\Delta\vec{G}, T\right)\cos\left(\Delta\vec{G}\cdot\vec{\tau}\right) + iW^a\left(\Delta\vec{G}, T\right)\sin\left(\Delta\vec{G}\cdot\vec{\tau}\right)$$

is the temperature dependent empirical local pseudopotential and $W^{s,a}(\Delta\mathbf{G}, T)$ are the symmetric, $W^s$ and antisymmetric, $W^a$ temperature dependent form factors, that are fitted empirically to obtain the required energy gap for the associated semiconductors (Si and Ge) and take the form [15]:

$$W^{s,A}\left(\Delta\vec{G}, T\right) = W^{s,a}\left(\Delta\vec{G}, T = 0\,K\right) - \Delta^{s,a}T, \quad (18)$$

where $\Delta^{s,a}$ are the temperature coefficient form factors.

The temperature dependent lattice constant, $a(T)$, which is determined from the relation [19]

$$a(T) = a(300\,K)[1 + \alpha_{th}(T - 300\,K)],$$

where $\alpha_{th}$ is the linear thermal expansion coefficient and its value that corresponding to the associated semiconductors

Si and Ge is listed in Table 6. The energy eigenvalues $E_{nk}(T)$ are calculated for different values of temperatures ranged from 0 to 500 K at constant $x$ and $P = 0$ kbar.

The experimental temperature energy gaps are obtained from Varshni's empirical formula as [33]

$$E_g(T) = E_g(0) - \frac{\alpha T^2}{T + \beta}.$$

The values of $\alpha$ and $\beta$ for the associated semiconductors Si and Ge are listed in Table 6.

The temperature dependent symmetric form factor parameters and the lattice constant associated with Si and Ge as functions of temperatures at $P = 0$ kbar are listed in Table 7. It is seen that the temperature dependent symmetric form factors are linearly decreasing functions with increasing the temperature. This is due to the fact that, raising temperature increases the dimension of the crystal, as observed from the variation of the lattice constant $a(T)$, which yields decreasing the potential energy seen by the electron.

Fig. 4 shows the electronic structure of $Si_{0.5}Ge_{0.5}$ as a function of the propagation wave vector $\mathbf{k}$ at $T = 0$ K (solid line) and $T = 500$ K (dashed line) at constant pressure $P = 0$ kbar. It is seen that the first conduction energy band is little slightly affected by temperature than the other bands. The energy differences between the calculated energy bands at $T = 0$ K and $T = 500$ K are about 0.1502 meV at point $\Gamma$, 11.8 meV at the point $L$, and 21 meV at the point $X$. All energy bands are showed little varying with increasing the temperature. It is seen that from Fig. 4 the effect of temperature on the energy band gaps is small; this means that this alloy is characterized by having high hardness, low compressibility, high ionicity, and high thermal conductivity. Such properties make it a good candidate for optoelectronic devices operating under extreme conditions [38].

**Table 6.** Values of the Varshni's parameters and the linear thermal expansion coefficients, and the pressure coefficients associated with the semiconductors used in these calculations [19]

| Parameters | Si | Ge |
|---|---|---|
| $\alpha$, $10^{-4}$ K$^{-2}$ | 4.730 | 4.800 |
| $\beta$, K | 636 | 235 |
| $\alpha_{\text{th}}$, $10^{-6}$, K$^{-1}$ | 2.616 | 5.75 |
| $c$, $10^{-2}$ eV/GPa | −1.43 | 4.80 |
| $d$, $10^{-4}$ eV/GPa$^2$ | 0.00 | 0.00 |
| $B$, GPa | 97.84 | 74.70 |
| $B'$ | 4.24 | 4.55 |

**Table 7.** The temperature dependence symmetric and antisymmetric form factor parameters for Si and Ge

| Form factors (Ryd) | $a$, $s$, $T \cdot 10^{-6}$ K$^{-1}$ | $T$ (K) 0 | 300 | 500 |
|---|---|---|---|---|
| Si | | | | |
| $W_3^s(T)$ | 0.0713333 | −0.2379777 | −0.2379991 | −0.2380134 |
| $W_8^s(T)$ | 0.022 | 0.0573077 | 0.0573011 | 0.0572967 |
| $W_{11}^s(T)$ | 0.001 | 0.0660302 | 0.0660299 | 0.0660297 |
| | | 5.4267378[m] | 5.4310000[m] | 5.4338415[m] |
| Ge | | | | |
| $W_3^s(T)$ | 0.0093333 | – | – | – |
| | – | 0.2995111 | 0.2995139 | 0.2995158 |
| $W_8^s(T)$ | 0.0043333 | 0.0774512 | 0.0774499 | 0.0774490 |
| $W_{11}^s(T)$ | 0.0016667 | 0.0017234 | 0.0017229 | 0.0017226 |
| | | 5.6481401[m] | 5.6579[m] | 5.6644066[m] |

*Note.* [m] Ref. [19].

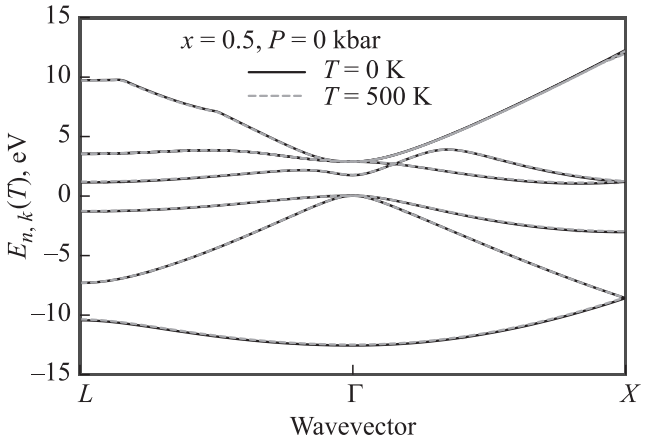


**Figure 4.** The electronic structure of $Si_{1-x}Ge_x$ at $P = 0$ kbar, $x = 0.5$ for two different values of temperatures: $T = 0$ K (solid line) and $T = 500$ K (dashed line).

### 3.3. Effect of pressure $P$ on $E_{nk}$ at constant composition $x$ and temperature $T$

For a given composition parameter $x$ and at constant temperature, $T = 300$ K, the pressure dependent eigenvalues and eigenvectors are found by solving the secular determinant.

$$\left\| \frac{1}{2}\left|\mathbf{k} + \mathbf{G}'\right|^2 - E_{nk}(P) + \sum_{G \neq G'} V\left(\left|\Delta\mathbf{G}\right|, P\right) \right\| = 0, \quad (19)$$

where

$$V\left(\left|\Delta\mathbf{G}\right|, P\right) = W^s\left(\Delta\mathbf{G}, P\right)\cos\left(\Delta\mathbf{G}\cdot\boldsymbol{\tau}\right) + iW^a\left(\Delta\mathbf{G}, P\right)\sin\left(\Delta\mathbf{G}\cdot\boldsymbol{\tau}\right)$$

is the pressure dependent empirical local pseudo-potential, $W^{s,a}(\Delta\mathbf{G}, P)$ are the pressure-dependent form factors of Si and Ge that are fitted empirically with the experimental values to obtain the best energy gap for the associated semiconductor which considered to take the form [16]

$$W^{s,a}(\boldsymbol{\tau}\Delta G, P) = W^{s,a}(\boldsymbol{\tau}\Delta G, P = 0) + \Delta^{s,a}P, \quad (20)$$

where $\Delta^{s,a}$ are the pressure coefficient form factors.

**Table 8.** The pressure dependence symmetric form factor parameters for Si and Ge at $T = 300$ K

| Form factors (Ryd) | $s$, $a$, $T$, $10^{-6}$ kbar | $P$ (kbar) 0 | 60 | 120 |
|---|---|---|---|---|
| Si | | | | |
| $W_3^s(P)$ | 0.0433333 | −0.2379991 | −0.2379965 | −0.2379939 |
| $W_8^s(P)$ | 0.02 | 0.0573011 | 0.0573035 | 0.0573059 |
| $W_{11}^s(P)$ | 86.5383333 | 0.0660299 | 0.0712222 | 0.0764145 |
| | | 5.4310000[m] | 5.3332089[m] | 5.2551267[m] |
| Ge | | | | |
| $W_3^s(P)$ | 0.04 | −0.2995139 | −0.2995115 | −0.2995091 |
| $W_8^s(P)$ | 0.0133333 | 0.0774499 | 0.0774507 | 0.0774515 |
| $W_{11}^s(P)$ | 22.1183333 | 0.0017229 | 0.0030500 | 0.0043771 |
| | | 5.6579[m] | 5.5302489[m] | 5.4349933[m] |

*Note.* [m] Ref. [19].

The experimental pressure dependent energy gaps are obtained from the empirical relation [19],

$$E_g^{d,id}(P) = E_g^{d,id}(0) + cP + dP^2, \qquad (21)$$

where $c$ and $d$ are the hydrostatic pressure coefficients listed in Table 6, $d$ and $id$ stand for direct and indirect energy bands.

The pressure dependence lattice constant has been estimated using the relation given by Adachi [19].

$$a(P) = a(0)\left[1 + \left(\frac{B'}{B}\right)P\right]^{-1/3B},$$

where $B$ is the bulk modulus, and $B'$ is the pressure derivative of the bulk modulus which are listed in Table 6, $a(0)$ and $a(P)$ are the lattice parameters at pressures $P = 0$ and $P \neq 0$, respectively.

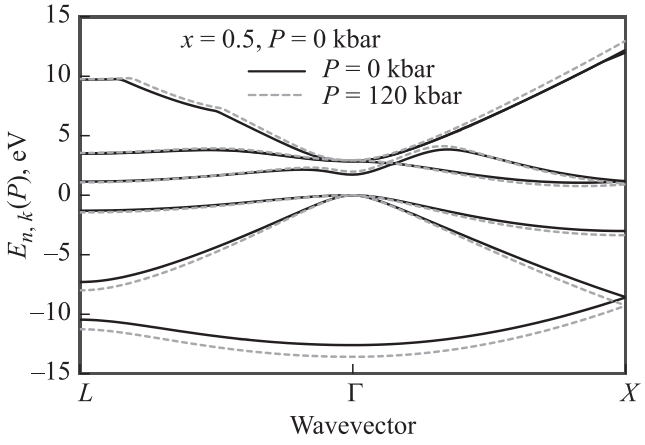


**Figure 5.** The electronic structure of $Si_{1-x}Ge_x$ at $T = 300$ K and $x = 0.5$ for two different values of pressures: $P = 0$ kbar (solid line) and $P = 30$ kbar (dashed line).

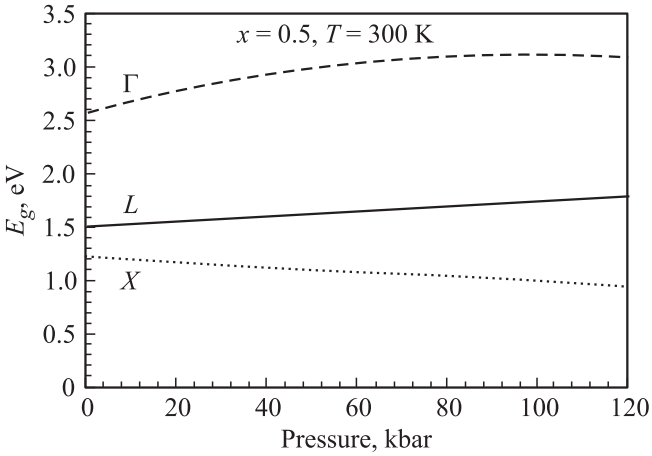


**Figure 6.** The direct and indirect energy band gaps for $Si_{1-x}Ge_x$ at $T = 300$ K, and $x = 0.5$.

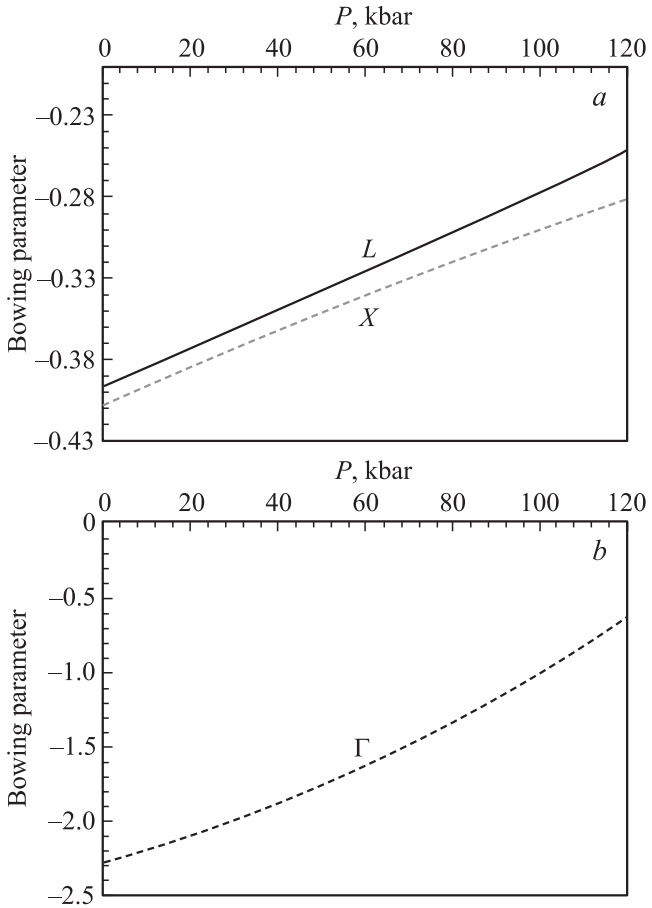


**Figure 7.** The bowing parameter for $Si_{1-x}Ge_x$ as a function of pressure.

The pressure dependent symmetric form factor parameters and the lattice constant associated with Si and Ge as functions of pressure from $P = 0$ to $P = 120$ kbar are listed in Table 8. It is seen from Table 8, that the pressure dependent symmetric form factors are linearly increasing functions with increasing the pressure. This is due to the

fact that, raising pressure decreases the dimension of the crystal, as observed from the variation of the lattice constant $a(P)$, which yields increasing the potential energy seen by the electron.

Fig. 5 displays the electronic structure of $Si_{0.5}Ge_{0.5}$ alloy as a function of the propagation wave vector $\mathbf{k}$ at $P = 0$ kbar (solid line) and $P = 120$ kbar (dashed line) at constant temperature $T = 300$ K. It is seen that the first conduction energy band is more affected by pressure than the others and exhibits more enhancement at the point Γ. The energy differences between the calculated electronic energies at $P = 0$ and $P = 120$ kbar are about 252.1 meV at point Γ, 39.2 meV at the point $L$, and 249.7 meV at the point $X$.

The dependence of the direct and indirect band gaps ($E_g^\Gamma$, $E_g^L$ and $E_g^X$) of the alloy $Si_{0.5}Ge_{0.5}$ at $T = 300$ K as a function of pressure is shown in Fig. 6. The energy bands are decreased with increasing the pressure at $X$ and $L$ points, but increased at Γ symmetry point.

The bowing parameter for the binary alloys energy gaps accounts the deviation from the linear interpolation, the so called virtual crystal approximation between the two binaries [39]. Fig. 7 show the bowing parameter as function of pressure at Γ, $X$ and $L$ symmetry points; we note that the bowing parameters are increased with increase the pressure from 0 up to 120 kbar at $L$ and $X$ points.

## 4. Conclusions

We have calculated the electronic band structure of $Si_{1-x}Ge_x$ alloy under the effects of composition $x$, temperature $T$, and pressure $P$ based on local empirical pseudo-potential method, and ignoring the non-local and the spin-orbit coupling effects. The temperature and pressure dependence of the pseudo-potential is performed by considering temperature and pressure linearly dependence of the pseudo-potential form factors, and the lattice constant. The calculations are performed under the virtual crystal approximation that takes into account the effect of compositional disorder. Temperature and pressure dependences of electronic band parameters for alloys $Si_{1-x}Ge_x$ have been investigated in the temperature range from 0 to 500 K and the pressure range from 0 to 120 kbar. The present results show good agreements with the experimental and published data.

Acknowledgments: Thanks for Prof. E.A. Elwakil, Head of theoretical group for various discussions and useful comments. Thanks also for Prof. A.M. Elabsy for his advising and encouragements.

## References

[1] M. Lopuszynski, J. Bartoszek, J.A. Majewski. Acta Phys. Polon. A, **112**, 2 (2007).
[2] J.C. Bean, L.C. Feldman, A.T. Flory, S. Harkahara, I.K. Robinson. J. Vac. Sci. Technol., **436**, A2 (1982).
[3] M.A. Gell. Phys. Rev. B, **38**, 7535 (1988).
[4] T.P. Pearsall, J. Bevk, L.C. Feldman, A. Ourmazd, J.M. Bornar, J.P. Mannaerts. Phys. Rev. Lett., **58**, 729 (1987).
[5] A.R. Degheidy, A.M. Elabsy, E.B. Elkenany. Superlat. Microstr., **52**, 336 (2012).
[6] A.R. Degheidy, E.B. Elkenany. Mater. Sci. Semicond. Proc., **15**, 505 (2012).
[7] G.A. Samara. Phys. Rev. B, **27**, 3494 (1983).
[8] B. Welber, M. Cardona, C.K. Kim, S. Rodriguez. Phys. Rev. B, **12**, 5729 (1975).
[9] H. Aourag, M. Ferhat, B. Bouhafs, N. Bouarissa, A. Zaoui, N. Amrane, B. Khelifa, Computational Mater. Sci., **3**, 393 (1995).
[10] Y.F.T. Say, B. Gong, S.S. Mitra, J.F. Vetelino. Phys. Rev. B, **6**, 2330 (1972).
[11] E.F. Skelton, P.L. Radoff, P. Bolsaitis, A. Verbalis. Phys. Rev. B, **5**, 3008 (1972).
[12] A.R. Degheidy, A.M. Elabsy, H.G. Abdelwahed, E.B. Elkenany. Indian. J. Phys., **86**, 363 (2012).
[13] R.N. Chan, M.L. Cohen. Phys. Rev. B, **1**, 2569 (1970).
[14] A. Gilat. MATLAB: *An Introduction with Applications*, 2nd edn. (Wiley, N.Y., 2005).
[15] A.M. Elabsy, E.B. Elkenany. Physica B, **405**, 266 (2010).
[16] A.M. Elabsy, A.R. Degheidy, H.G. Abdelwahed, E.B. Elkenany. Physica B **405**, 3709 (2010).
[17] A.R. Degheidy, E.B. Elkenany. Semiconductors, **45**, 10 (2011).
[18] P. Harrison. *Quantum Wells Wires and Quantum Dots*, 2nd edn. (Wiley, N.Y. 2005) chap. 11.
[19] S. Adachi. Properties of Group-IV, III–V and II–VI Semiconductors (Wiley, N.Y., 2005) chap. 2.
[20] S.J. Lee, T.S. Kwon, K. Nahm, C.K. Kim. J. Phys. Condens. Matter, **2**, 3253 (1990).
[21] N. Bouarissa. Phys. Lett. A, **245**, 285 (1998).
[22] N. Bouarissa, H. Aourag. Phys. Status Solidi B, **190**, 227 (l995).
[23] L. Vegard. Z. Phys., **5**, 17 (1921).
[24] S. Abdi-Ben Nasrallah, S. Ben Afia, H. Belmabrouk, M. Said. Eur. Phys. J. B, **43**, 3 (2005).
[25] T.S. Moss. Phys. Status Solidi B, **131**, 415 (1985).
[26] N.M. Ravindra, V.K. Srivastava. Infr. Phys., **19**, 603 (1979).
[27] V.P. Gupta, N.M. Ravindra. Phys. Status Solidi B, **100**, 715 (1980).
[28] P.J.L. Herve, L.K.J. Vandamme. Infr. Phys. Technol., **35**, 609 (1994).
[29] C. Kittel. *Introduction to solid state physics*, 8th edn (Wiley, Sons, Inc., 2005).
[30] J. Weber, M.I. Alonso. Phys. Rev. B, **40**, 5683 (1989).
[31] O. Madelung, ed. *Numerical data and functional relationships in science and technology*, Group III (Springer, Berlin, 1982).
[32] R. Braunstein, A.R. Moore, F. Herman. Phys. Rev., **109**, 695 (1958).
[33] Y.P. Varshni. Physica, **34**, 149 (1967).
[34] P.E. Batson, J.F. Mrad. Appl. Phys. Lett., **58**, 3285 (1991).
[35] S. Kristhnamurthy, A. Sher, A.B. Chen. Phys. Rev. B. **33**, 1026 (1986).
[36] S. Kristhnamurthy, A. Sher, A.B. Chen. Phys. Rev. Lett., **55**, 320 (1985).
[37] K.E. Newman, J.D. Dow. Phys. Rev. B, **30**, 1929 (1984).
[38] T. Lei, T.D. Moustakas, R.J. Graham, Y. He, S.J. Berkowitz. J. Appl. Phys., **71**, 4933 (1992).
[39] I. Vurgaftman, J.R. Meyer, L.R. Ram-Mohan. J. Appl. Phys., **89**, 5815 (2001).

*Редактор Т.А. Полянская*